

Natural ventilation of multiple storey buildings: The use of stacks for secondary ventilation

Stephen R Livermore*, Andrew W Woods

BP Institute for Multiphase flow, University of Cambridge, Cambridge CB3 0EZ, UK

Received 17 August 2004; received in revised form 19 April 2005; accepted 18 May 2005

Abstract

The natural ventilation of buildings may be enhanced by the use of stacks. As well as increasing the buoyancy pressure available to drive a flow, the stacks may also be used to drive ventilation in floors where there is little heat load. This is achieved by connecting the floor with a relatively low heat load to a floor with a higher heat load through a common stack. The warm air expelled from the warmer space into the stack thereby drives a flow through the floor with no heat load. This principle of ventilation has been adopted in the basement archive library of the new SSEES building at UCL. In this paper a series of laboratory experiments and supporting quantitative models are used to investigate such secondary ventilation of a low level floor driven by a heat source in a higher level floor. The magnitude of the secondary ventilation within the lower floor is shown to increase with the ratio of the size of the openings on the lower to the upper floor and also the height of the stack. The results also indicate that the secondary ventilation leads to a reduction in the magnitude of the ventilation through the upper floor, especially if the lower floor has a large inlet area. © 2005 Elsevier Ltd. All rights reserved.

Keywords: Natural ventilation; Stacks; Secondary ventilation; Buoyancy

1. Introduction

There is increasing awareness of the high energy consumption in buildings. Many buildings use mechanical air conditioning to regulate the internal environment, but even with energy efficient designs, they typically use around 230 KWh/m² of energy [1]. However, in a number of buildings, alternative low energy systems use natural ventilation to significantly reduce the energy consumption. Research has developed a good understanding of the basic principles of natural ventilation [2–4] within simple building structures. One of the key challenges now, is concerned with understanding the subtleties of such flows within more complex multiple storey buildings.

A particular challenge associated with naturally ventilating large office spaces is the provision of

ventilation for areas in which there is insufficient buoyancy to drive a flow. A possible solution for this is through the use of stacks to couple floors with large heat loads to those without. In this manner, the warm air expelled into a stack from a space with a large heat load may be used to drive a flow on a different floor which otherwise would have insufficient buoyancy to drive a ventilation flow (Fig. 1). In this work, the impact of a stack on the upwards buoyancy driven displacement flow of a room with a heated floor is reviewed and referred to as the *primary* ventilation flow. These principles are then used to investigate how *secondary* ventilation flows can be induced on a floor located beneath the primary heated floor through the use of common stacks.

This type of ventilation may be of use in an office or industrial environment in which there is a low occupancy zone at low level. Indeed such a scheme is being implemented for the ventilation of the basement library in the new SSEES building at UCL [5]. In a different

*Corresponding author. Tel.: +44 1223 765711.

E-mail address: Stephen@bpi.cam.ac.uk (S.R. Livermore).

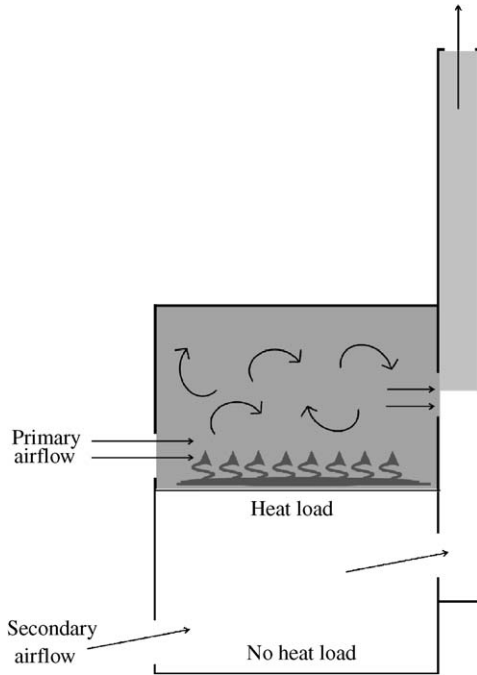


Fig. 1. Heat load on the upper floor driving the primary ventilation flow. By coupling the two floors with a common stack, the warm primary flow may be used to induce a secondary ventilation flow on the lower floor.

implementation of the concept, a warehouse could be ventilated through the use of offices located at an elevated height within the space. As well as ventilating lower level floors of minimal heat load, the scheme could also be used to enhance night or evening cooling of thermal mass in an undercroft, in for example, theatres. In this work, attention is restricted to the case of upward displacement ventilation, although it is noted that where multiple stacks are employed it is possible for some of the stacks to witness downward flow [6].

The paper is organised as follows. In Section 2, a steady state model is presented for a single room connected to high level stacks. The focus here is on the pressure losses associated with different inflow designs to the stacks and also the frictional losses within the stacks. In Section 3, a small scale analogue laboratory experiment is described which is used to validate the model. The principles developed for a single room are then applied in Section 4 to describe the coupled flow on two different floors which are connected by common stacks. Analogue experiments are conducted to test and validate the model of the flow in a two storey model building. In Section 6 the results are applied to a typical building geometry to provide simple guidelines for the designers of naturally ventilated buildings. Note all physical properties and dimensionless numbers are defined in Appendix A.3, the variables used in the single floor analysis are given in

Appendix A.4 and those for the two floor analysis in Appendix A.5.

2. Theoretical model

Consider a single room of height H connected to a stack of height x (Fig. 2). The room contains a distributed heat source, Q_H resulting from people, office equipment and solar radiation which drives an upwards displacement ventilation flow. It is assumed that the Rayleigh number, Ra of the air is high [7], such that the air is well-mixed [3]. The air enters through a low level opening of area A_L and exits by flowing horizontally into the stack entrance of area A_U (Fig. 2 (a)) before rising and flowing out to the ambient.

For a room with high and low level vents operating under displacement ventilation, the steady state volume flux is determined by pressure and energy balances within the room [2,8]. The former is a balance between the driving pressure, i.e. the difference in hydrostatic pressure between the interior and ambient, and the pressure losses which the flow encounters

$$\Delta\rho g(H + x) = \sum P_{\text{loss}}, \tag{1}$$

where $\Delta\rho = \rho - \rho_E$. The energy balance is given by equating the heat gains to the room, Q_H , with the advection of heat associated with the ventilation flow and the heat loss through the walls:

$$Q_H = \rho C_p Q \Delta T + U A_R \Delta T, \tag{2}$$

where Q is the volume flux and U and A_R are the heat transfer coefficient and surface area of the walls respectively and $\Delta T = T - T_E$ is the temperature difference between the interior and ambient.

For small temperature differences, the variations in density and temperature are linearly related [9] according to

$$\Delta\rho = \rho\alpha\Delta T, \tag{3}$$

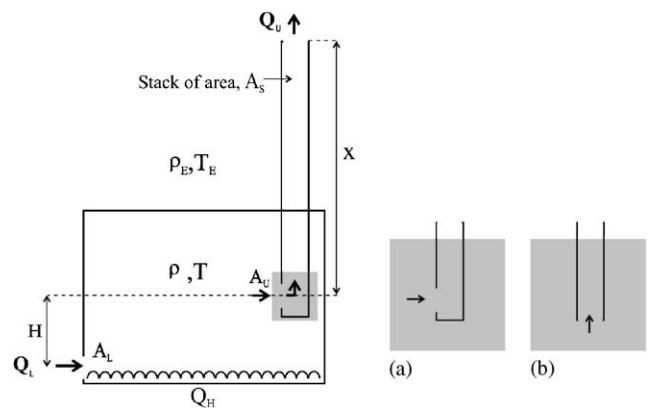


Fig. 2. Schematic of single room containing a distributed heat source Q_H connected to a single high level stack with (a) horizontal stack entry (b) vertical stack entry.

where α is the thermal expansion coefficient of air. These three equations may be combined to give the steady state volume flux and temperature as a function of the prescribed heat load, Q_H .

In calculating the pressure losses associated with the flow it is necessary to include the loss through the lower opening ΔP_L and the loss through the stack entrance, ΔP_U . In addition, this model also considers the pressure loss required to accelerate the flow round any corners in the stack, ΔP_M and the frictional loss in the main up flow within the stack, $\Delta P_{friction}$. In this present work it is assumed that there is no additional pressure loss encountered as the flow exits at the top of the stack.

2.1. Loss through openings, $\Delta P_{openings}$

Following Linden et al. [10] the pressure losses through the inflow and outflow openings are given in terms of the volume flux, Q_i , by

$$\Delta P_i = \frac{\rho u_i^2}{2c_i^2} = \frac{\rho Q_i^2}{2c_i^2 A_i^2}, \quad i = L, U, \quad (4)$$

where c_i and A_i are the discharge coefficient and opening areas respectively and the subscripts, L and U refer to the lower and stack openings. In practice, the design of the stack entry will influence the magnitude of the discharge coefficient of the flow into the stack. For simplicity it is assumed that the entry into the stack will act as a localised opening in the same manner as the lower inlet opening A_L . As such a constant value of $c_i = c = 0.7$ [11] will be used for all openings throughout this work.

By mass conservation the volume flux entering at low level, Q_L is equal to that leaving at high level, Q_U such that $Q_L = Q_U = Q$.

2.2. Loss in stack turning, ΔP_M

If, for example, the air flows into the stack horizontally but then turns to flow vertically upwards as shown in Fig. 2(a), the associated vertical acceleration causes a reduction in the pressure, ΔP_M . This pressure loss is given by a vertical momentum balance on the control volume shown in Fig. 3. Here, the stack is closed below the level of the inlet and it is assumed that the pressure on the closed damper, P_D is equal to P_U , the pressure just inside the stack opening (c.f. Batchelor [12]). The reduction in pressure across the control volume is therefore given by $\Delta P_M = P_D - P_S$ where P_S is the pressure in the stack above the control volume.

$$A_S \Delta P_M = \dot{m}u = \rho A_S u^2, \quad (5)$$

$$\Rightarrow \Delta P_M = \rho u^2 = \rho \left(\frac{Q}{A_S} \right)^2, \quad (6)$$

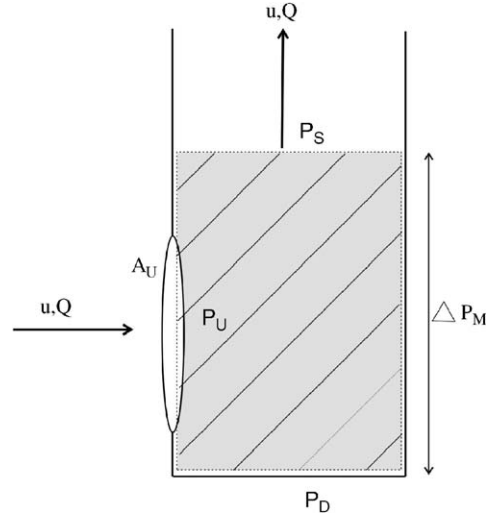


Fig. 3. Control volume analysis at the base of the stack. It is assumed that $P_U = P_D$ such that the vertical acceleration is associated with the pressure difference, $\Delta P_M = P_D - P_S$.

where A_S is the area of a single stack and \dot{m} and u are the mass and velocity flux up the stack respectively.

2.3. Frictional loss in stack, $\Delta P_{friction}$

The frictional pressure loss in a circular stack of length x and radius r is given following Ward-Smith [13]:

$$\Delta P_{friction} = \frac{fx}{r} \rho u^2. \quad (7)$$

Here f is the friction factor and is determined separately according to whether the flow is turbulent or laminar. The Reynolds number is the important parameter to consider in this case:

$$Re = \frac{ud}{\nu}, \quad (8)$$

where d is the diameter of the stack and ν is the kinematic viscosity. For example, with a ventilation flow rate of $1 \text{ m}^3/\text{s}$, the speed in a stack of diameter 0.5 m would be $u \sim 5 \text{ m/s}$ and the associated $Re \sim 10^5$. It is anticipated that the flow within the stack will have large Re and hence f is given by the Blasius formula [13]:

$$f = 0.079 Re^{-0.25}. \quad (9)$$

For a stack height of 10 m , substituting Eq. (9) into Eq. (7) and using $Re = 10^5$ gives

$$\Delta P_{friction} \sim 0.2 \rho u^2. \quad (10)$$

This can be compared to the pressure loss at the openings. Combining both the inlet and outlet vents the pressure loss is given by (4) as

$$\Delta P_{openings} \sim 2 \rho u^2, \quad (11)$$

which is a factor of 10 greater than $\Delta P_{\text{friction}}$. Therefore the pressure loss resulting from friction within the stacks is only of secondary importance compared to the pressure losses at the openings and that due to the momentum change within the stack. Consequently it can be omitted from the model.

2.3.1. Pressure and energy balances

By combining Eqs. (1), (4) and (6) the pressure balance for the case of *one* stack is given by the relation

$$\Delta\rho g(H+x) = \rho Q^2 \left(\frac{1}{2c^2 A_L^2} + \frac{1}{2c^2 A_U^2} + \frac{1}{A_S^2} \right), \quad (12)$$

which can be rearranged into the form

$$Q = A^* \left(\frac{\Delta\rho}{\rho} g(H+x) \right)^{1/2}. \quad (13)$$

Here A^* is the effective area given by

$$A^* = \frac{\sqrt{2c} A_L A_U A_S}{\sqrt{2c^2 A_L^2 A_U^2 + A_L^2 A_S^2 + A_U^2 A_S^2}}. \quad (14)$$

If it is assumed that the room is well insulated, the heat loss through the walls will be negligible compared with the heat lost by advection through the openings. The steady state ventilation flow, Q is given in terms of a prescribed heat flux, Q_H as

$$Q = A^{*2/3} \left(\frac{g\alpha Q_H (H+x)}{\rho C_p} \right)^{1/3}. \quad (15)$$

3. Experiments

3.1. Apparatus

In order to test the model, an analogue experiment has been developed similar to that employed by Chenvidyakarn and Woods [6]. The apparatus has two floors connected to a series of stacks. Each floor consists of a 1 cm thick acrylic tank of inner dimensions $17.5 \times 17.5 \times 10$ cm. Both floors contains five low level openings of 1.5 cm diameter, positioned with their mid-points 1.5 cm above the base. In addition, five stacks of 1.35 cm internal diameter and 35 cm total length are located at the end opposite the openings. These contain horizontal openings also of diameter 1.35 cm which act as mid-level outflow vents for the room.

The upper floor (denoted hereafter as the second floor) contains a distributed heating wire of power output 0–500 W designed to provide a uniform source of buoyancy. This is connected to a 30 V transformer via voltage and current meters which allows the power

output to be accurately measured. Ten type K shielded thermocouples are used to measure the temperature at various positions within the model. Four of these are located in the room at heights 3, 5, 7 and 9 cm from the floor base and four are positioned within the centre stack at 5, 10, 15 and 20 cm above the upper floor outflow vent. In addition two thermocouples are kept in the ambient water to ensure this remains constant throughout the experiment. The thermocouples take a measurement every second and the data feeds into a PC via a Picotech TC08 cold junction.

3.2. Method

For the single floor experiments, the first floor is sealed off with rubber bungs (Fig. 4) and only the second floor is considered. To commence an experiment, the tank is filled with cold water of temperature typically in the range 14–17 °C. The average temperature is recorded and used as a reference with which to calibrate all the thermocouples. When the heating is initiated, thermal plumes are seen to rise from the wire and the temperature within the room increases. Within a few seconds this warm water begins to flow into the stacks where it rises and flows out to the ambient. The temperature increases until steady state conditions are reached, typically after around 20 min (Appendix A.2). For the first series of experiments; the area of the second floor inflow opening $A_L = 3.5 \text{ cm}^2$ and $Q_H = 450 \text{ W}$ and these are kept constant throughout, whilst the number of stacks, n is varied between one and five. As the number of stacks is increased, the steady state temperature falls off very sharply owing to the increased available area and the greater ventilation flow that results (Fig. 5).

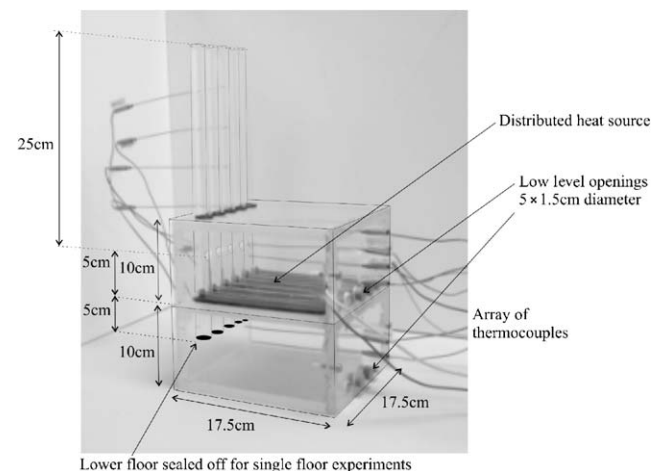


Fig. 4. The apparatus comprises of two floors connected by common stacks. For this initial study the first floor has been sealed off and removed from operation.

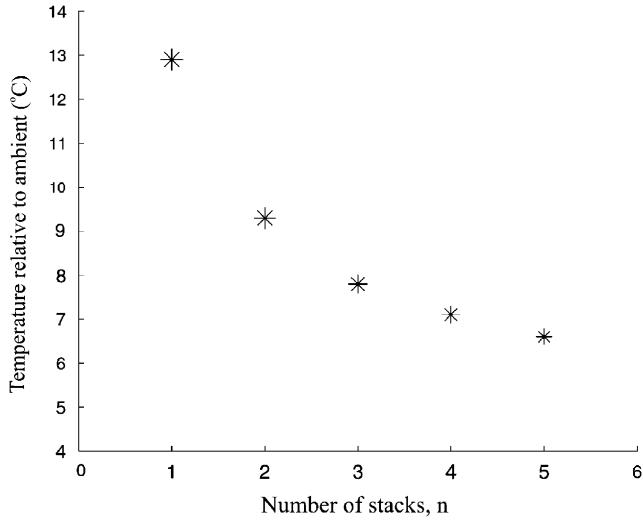


Fig. 5. Steady State temperature relative to ambient as a function of the number of stacks, n with $Q_H = 450$ W and $A_L = 3.5$ cm², indicating that initially increasing the number of stacks decreases the temperature but when $n > 3$ it has significantly less impact.

3.3. Adapting the model for comparison with the experiments

In the analogue experiments it is found that velocities of order 10^{-1} – 10^{-2} ms⁻¹ develop in the stacks, leading to $Re \sim 1000$. Such flow is laminar and the friction factor may be given by Fanning [13] as

$$f = \frac{16}{Re}. \quad (16)$$

In this case, $\Delta P_{\text{friction}} \sim \rho u^2$ while $\Delta P_{\text{openings}} \sim 2\rho u^2$ and consequently it is necessary to include $\Delta P_{\text{friction}}$ in the model. Substituting Eq. (16) into Eq. (7) gives the frictional pressure loss as

$$\Delta P_{\text{friction}} = \frac{8\pi v \rho x}{A_S^2} \left(\frac{Q}{n} \right), \quad (17)$$

where it is assumed that the velocity flux through each stack is $\frac{Q}{n}$. The overall pressure balance for the analogue model incorporating n stacks is then given by combining Eq. (17) with Eq. (12):

$$\Delta \rho g(H+x) = \rho Q^2 \left(\frac{1}{2c^2 A_L^2} + \frac{1}{2c^2 (nA_U)^2} + \frac{1}{(nA_S)^2} \right) + \frac{8\pi v \rho x}{A_S^2} \left(\frac{Q}{n} \right). \quad (18)$$

Eq. (2) can be rearranged to give the temperature difference between the interior and ambient as

$$\Delta T = \frac{Q_H}{\rho C_p Q + UA_R}, \quad (19)$$

where A_R is the surface area of the floor in contact with the ambient water. Eqs. (3), (18) and (19) can be combined to obtain the governing steady state equation

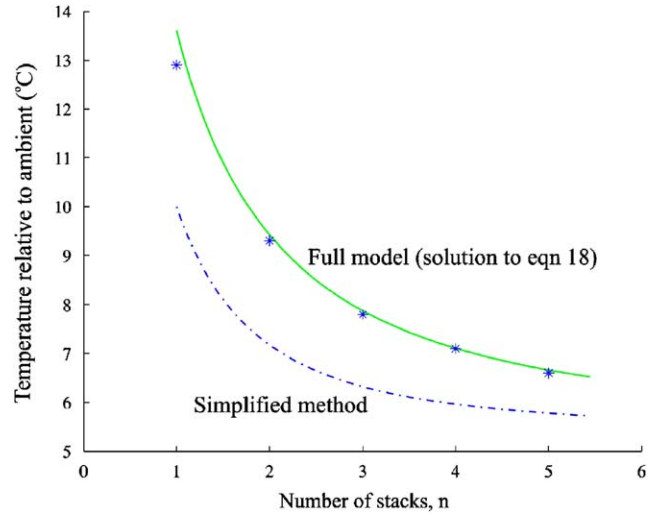


Fig. 6. Comparison of experiments (stars) with theory (lines). The model developed in Section 3.3 is shown by the solid line and the simplified model which neglects ΔP_M and $\Delta P_{\text{friction}}$ is shown by the dotted line. In this experiment $A_L = 3.5$ cm² and $Q_H = 450$ W.

for this flow

$$\frac{\alpha g(H+x)Q_H}{\rho C_p Q + UA_R} = Q^2 \left(\frac{1}{2c^2 A_L^2} + \frac{1}{2c^2 (nA_U)^2} + \frac{1}{(nA_S)^2} \right) + \frac{8\pi v x}{A_S^2} \left(\frac{Q}{n} \right). \quad (20)$$

Eq. (20) can be solved to find the volume flux, Q . This can then be substituted back into (19) to give the temperature excess at steady state. To compare the experimental results with the predictions of the steady state model, it is necessary to determine the value of the heat transfer coefficient, U for the analogue system. To this end, transient cooling experiments, described in Appendix A.1 have been used to show $U = 13$ W/m²k. In Fig. 6 the predictions of Eq. (20) are compared with the experimental measurements and are shown to be in close agreement. The importance of including the pressure loss associated with change in flow direction in the stack, ΔP_m and also the frictional pressure losses along the stacks, $\Delta P_{\text{friction}}$ can be seen from the dotted line which corresponds to the theoretical predictions which ignore these effects.

4. Two floors connected by a common stack

The method developed in Section 2 is now extended to model the ventilation through the two floor building shown in Fig. 7. In this case, the second floor contains an evenly distributed heat source and the first floor, which is connected to the second floor via common stacks, contains no appreciable source of heating. The floors have inflow openings of size A_{1L} and A_{2L} . In addition a series of n stacks each of cross-sectional area,

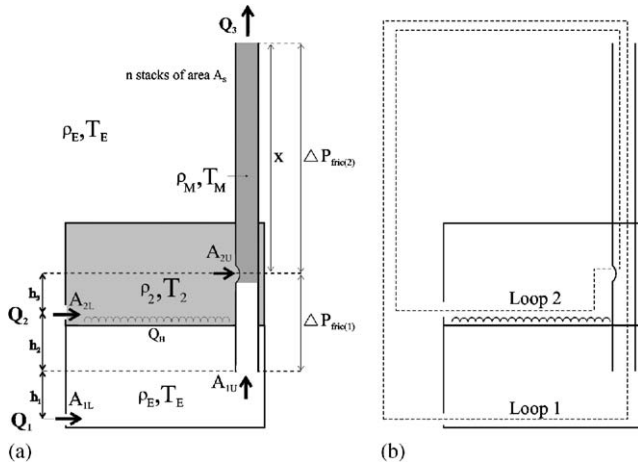


Fig. 7. (a) Schematic of simple two floor model with heat flux in second floor only, (b) Closed loops used for the pressure analysis, loop 1 refers to the pressure losses on the first floor and loop 2 to the losses on the second floor.

A_S and total height $x + h_2 + h_3$ are positioned on the opposite side of the building. These protrude down through the second floor to provide mid-level outflow vents for the first floor. The outflow vents for the first and second floors have areas A_{1U} and A_{2U} in each stack respectively and thus total areas of nA_{1U} and nA_{2U} where there are n open stacks.

The warm air in the second floor at temperature, T_2 will tend to flow into the stacks where it will rise and exit to the exterior. The warm air within the stacks will induce a secondary flow in the first floor, drawing in ambient air through A_{1L} . This air will flow into the stacks where it will mix with the outflow from the second floor. It is assumed that this mixing occurs instantaneously at the upper floor inlet such that the air above the point of mixing can be assumed to be at the uniform temperature, T_M , a mean temperature of T_2 and the ambient temperature, T_E from the first floor, weighted according to the volume fluxes, Q_1 and Q_2 through the first and second floors respectively. To determine these volume fluxes pressure balances are considered around flow loops 1 and 2 shown in Fig. 7(b).

Loop 1, for the first floor:

$$(\rho_M - \rho)gx = \Delta P_{1L} + \Delta P_{1U} + \Delta P_{M(2)} + \Delta P_{fric(1)} + \Delta P_{fric(2)} \quad (21)$$

and loop 2, for the second floor:

$$(\rho_2 - \rho)gh_3 + (\rho_M - \rho)gx = \Delta P_{2L} + \Delta P_{2U} + \Delta P_{M(2)} + \Delta P_{fric(2)}, \quad (22)$$

where ΔP_{1L} and ΔP_{2L} are the pressure losses through the low level openings A_{1L} and A_{2L} respectively, and ΔP_{1U} and ΔP_{2U} are the losses into the stacks through A_{1U} and A_{2U} . The pressure loss associated with the change in direction of the flow as it enters the stack from

the second floor is given by $\Delta P_{M(2)}$. In this two floor model, the frictional loss in the stacks is divided into two parts, that seen below the second floor inlet, $\Delta P_{fric(1)}$ and that above the inlet, $\Delta P_{fric(2)}$.

Since the lower floor contains no source of heating, an energy balance is only required on the upper floor. By applying Eq. (2) this is given by

$$Q_H = \rho C_p Q_2 (T_2 - T_E) + UA_R (T_2 - T_E). \quad (23)$$

4.1. Pressure loss at stack inflow on second floor, $\Delta P_{M(2)}$

In a similar manner to Section 4.1, there will be a reduction in pressure associated with accelerating the flow vertically at the second floor stack entry. In this case, however, the upward flow from the first floor, Q_1 also needs to be considered. As before, the analysis is simplified by assuming that the pressure on the internal side of A_{2U} is equal to that at the base of the control volume, P_D . To calculate the reduction in pressure, $\Delta P_{M(2)}$ ($= P_D - P_S$), between the base and top of the control volume, P_S , mass and momentum balances are considered as follows (Fig. 8):

$$Q_1 + Q_2 = Q_3, \quad (24)$$

$$A_S \Delta P_{M(2)} = \{\dot{m}u\}_{out} - \{\dot{m}u\}_{in} = \rho A_S (u_3^2 - u_1^2). \quad (25)$$

Substituting Eq. (24) into Eq. (25) the pressure loss for one stack can be calculated as

$$\begin{aligned} \Delta P_{M(2)} &= \rho(u_3^2 - u_1^2) = \frac{\rho}{(A_S)^2} (Q_3^2 - Q_1^2) \\ &= \frac{\rho}{(A_S)^2} (Q_2^2 + 2Q_1 Q_2), \end{aligned} \quad (26)$$

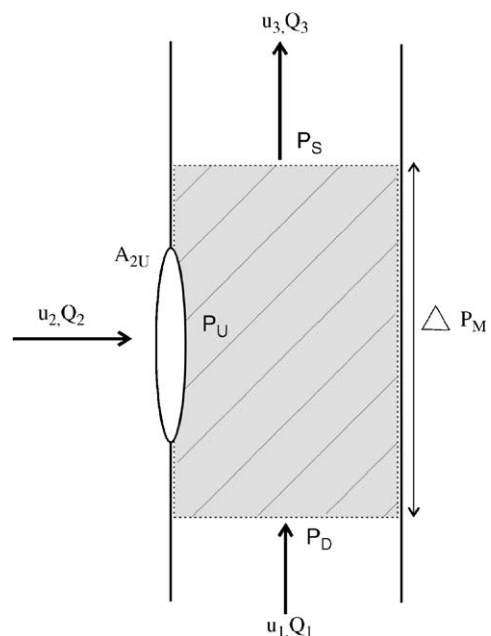


Fig. 8. Control volume around upper floor stack inlet.

where u_1 and u_2 are the velocity fluxes and Q_1 and Q_2 the volume fluxes through the first and second floors, respectively. The volume flux through the upper section of the stacks is given by Q_3 . Following the analysis of Section 2.3 the pressure losses, $\Delta P_{\text{fric}(1)}$ and $\Delta P_{\text{fric}(2)}$ can be ignored when analysing the full air driven case. The pressure balances for n stacks can therefore be expressed as follows.

For loop 1, corresponding to the flow on the first floor

$$(\rho - \rho_M)gx = \rho Q_1^2 \left(\frac{1}{2c^2 A_{1L}^2} + \frac{1}{2c^2 (nA_{1U})^2} \right) + \frac{\rho}{(nA_S)^2} (Q_2^2 + 2Q_1 Q_2) \quad (27)$$

and for loop 2, corresponding to the flow on the second floor:

$$(\rho - \rho_2)gh_3 + (\rho - \rho_M)gx = \rho Q_2^2 \left(\frac{1}{2c^2 A_{2L}^2} + \frac{1}{2c^2 (nA_{2U})^2} \right) + \frac{\rho}{(nA_S)^2} (Q_2^2 + 2Q_1 Q_2). \quad (28)$$

Combining Eqs. (27) and (28) with (23), two coupled nonlinear relations are obtained for the flow on each floor in terms of the heat load Q_H :

$$\frac{\alpha g x Q_2 Q_H}{(Q_1 + Q_2)(\rho C_p Q_2 + U A_R)} = Q_1^2 \left(\frac{1}{2c^2 A_{1L}^2} + \frac{1}{2c^2 (nA_{1U})^2} \right) + \frac{Q_2^2 + 2Q_1 Q_2}{(nA_S)^2}, \quad (29)$$

$$\frac{\alpha g x Q_2 Q_H}{(Q_1 + Q_2)(\rho C_p Q_2 + U A_R)} + \frac{\alpha g h_3 Q_H}{\rho C_p Q_2 + U A_R} = Q_2^2 \left(\frac{1}{2c^2 A_{2L}^2} + \frac{1}{2c^2 (nA_{2U})^2} \right) + \frac{Q_2^2 + 2Q_1 Q_2}{(nA_S)^2}. \quad (30)$$

These have been solved numerically using the Newton Raphson method (see for example [14] for an appropriate technique) and the results are analysed in Section 6.

5. Experiments

Analogue experiments were conducted on the two floor model using the apparatus described in Section 3. In this case, the stacks have been opened up so that they protrude down through the second floor and provide mid-level outflow vents for the first floor. The first floor has the same dimensions as the second floor and also contains five low level openings each of 1.5 cm diameter, which allows the dependence of the secondary flow on the first floor inflow area to be explored. Two additional

thermocouples are positioned in the first floor to measure the temperature of the water inflowing through this floor.

5.1. Observations

A photograph of a typical experiment is shown in Fig. 9. In this experiment, one stack is used for the common outflow and on each floor two inflow vents are opened so that $A_{1L} = A_{2L} = 3.5 \text{ cm}^2$. Prior to the experiment the first floor is filled with dye. The experiment is started by applying a steady heat flux of 450 W to the second floor. On initiation of the heat flux the dye is drawn upwards through the stack. Above the first floor stack inlet, however, the colour is diluted by the entry of flow from the second floor. Above this level the fluid is a mixture of ambient water from the lower floor and warm water from the second floor.

Steady state conditions for each experiment are typically reached in around 20 min (Appendix A.2), depending on the restriction of the openings and the magnitude of the heat flux applied to the model. A typical plot of the temperatures within the stack and second floor relative to the exterior is shown in Fig. 10. At steady state the stack temperature $T_M < T_2$, owing to the inflow from the first floor. The temperatures recorded in the stack are significantly more variable than those for the second floor. This may be a result of the fact that the full mixing of the two streams requires a distance along the stack of order 3–4 stack diameters. Consequently, a number of the thermocouples in the

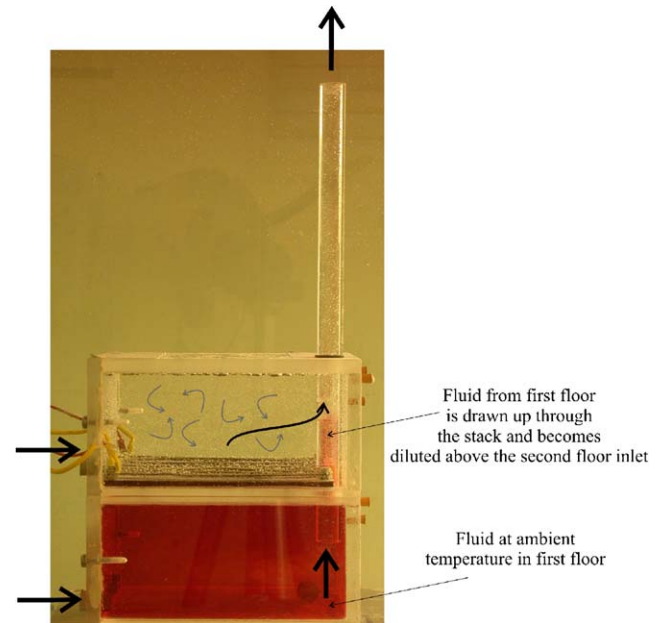


Fig. 9. Shadowgraph showing ambient water from the lower floor (dyed) being drawn upwards through the stack. For this experiment, $A_{1L} = A_{2L} = 3.5 \text{ cm}^2$, $n = 1$ and $Q_H = 450 \text{ W}$.

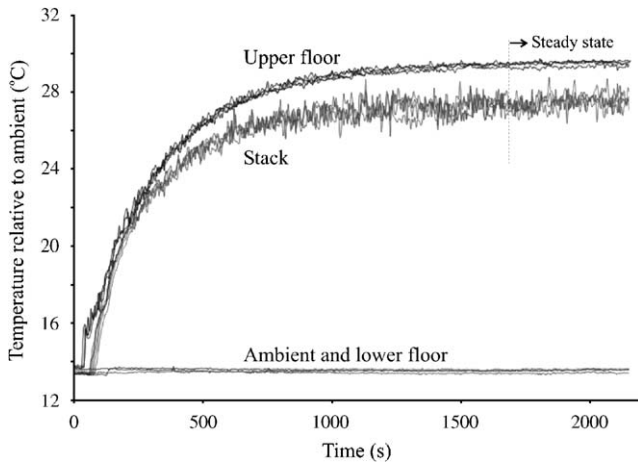


Fig. 10. Transient temperature data for one stack, $A_{1L} = A_{2L} = 3.5 \text{ cm}^2$.

stack are located within the mixing region leading to considerable fluctuations in the temperature measurement. However the time period of oscillation is very low and indeed significantly smaller than the time required for the water to rise out of the stack. We can infer from this, therefore, that an approximate well-mixed model may provide a leading order description for the bulk dynamics although point measurements of temperature may be subject to fluctuations. In comparing the model predictions with the experiments, the temperature measurements were averaged over a period of 100 s.

5.2. Adapting the model for comparison with experiments

As in Section 3.3, to compare the model with the analogue experiments the frictional loss within the stacks needs to be included. Eq. (17) is therefore substituted into Eqs. (21) and (22) to give the pressure balance for the first floor as

$$(\rho - \rho_M)gx = \rho Q_1^2 \left(\frac{1}{2c^2 A_{1L}^2} + \frac{1}{2c^2 (nA_{1U})^2} \right) + \frac{8\pi v \rho}{A_S^2} \left\{ \frac{Q_1}{n} (h_2 + h_3) + \frac{(Q_1 + Q_2)}{n} x \right\} + \frac{\rho}{(nA_S)^2} (Q_2^2 + 2Q_1 Q_2) \quad (31)$$

and for the second floor as

$$(\rho - \rho_2)gh_3 + (\rho - \rho_M)gx = \rho Q_2^2 \left(\frac{1}{2c^2 A_{2L}^2} + \frac{1}{2c^2 (nA_{2U})^2} \right) + \frac{8\pi v \rho (Q_1 + Q_2)}{A_S^2} x + \frac{\rho}{(nA_S)^2} (Q_2^2 + 2Q_1 Q_2). \quad (32)$$

Combining Eqs. (31) and (32) with Eq. (23) the coupled nonlinear relations have the form

$$\frac{\alpha g x Q_2 Q_H}{(Q_1 + Q_2)(\rho C_p Q_2 + UA_R)} = Q_1^2 \left(\frac{1}{2c^2 A_{1L}^2} + \frac{1}{2c^2 (nA_{1U})^2} \right) + \frac{8\pi v}{A_S^2} \left\{ \frac{Q_1}{n} (h_2 + h_3) + \frac{(Q_1 + Q_2)}{n} x \right\} + \frac{Q_2^2 + 2Q_1 Q_2}{(nA_S)^2}, \quad (33)$$

$$\frac{\alpha g x Q_2 Q_H}{(Q_1 + Q_2)(\rho C_p Q_2 + UA_R)} + \frac{\alpha g h_3 Q_H}{\rho C_p Q_2 + UA_R} = Q_2^2 \left(\frac{1}{2c^2 A_{2L}^2} + \frac{1}{2c^2 (nA_{2U})^2} \right) + \frac{8\pi v (Q_1 + Q_2)}{A_S^2} x + \frac{Q_2^2 + 2Q_1 Q_2}{(nA_S)^2}, \quad (34)$$

which again have been solved numerically [14].

5.3. Results

As Fig. 11 shows, the model predictions for the temperature of the second floor are in good accord with the experimental data. Here the temperatures within both the second floor and stacks (relative to the ambient) are shown as a function of the number of stacks. The low level inflow vents for both floors have area $A_{1L} = A_{2L} = 3.5 \text{ cm}^2$. On the other hand, the time averaged temperature measured within the stack is systematically higher than the model predictions by about $20 \pm 10\%$. This is likely to be due to the inefficient mixing of the two flows within the stack. Despite this, however, owing to the close match between the theory and experiments in the second floor, the bulk buoyancy provided by the stacks is likely to be consistent with that predicted by the leading order model. The effect of variations in the inflow area in the second floor, A_{2L} on the temperature in the second floor are shown in Fig. 12. Here the inflow area for the first floor has the fixed value of $A_{1L} = 3.5 \text{ cm}^2$ (corresponding to two openings). The results are shown for the cases of two and four stacks.

6. Application of model

The results from the model developed in Section 4 are now applied to illustrate some principles for the designers of naturally ventilated buildings. Consider a simple example comparable to the SSEES building at UCL [5], where the basement archive library of low occupancy, is ventilated by connecting to the ground floor containing a heat load of 3 KW. In this two floor model comprising of the basement and ground floor, each floor is 3 m high such that $h_1 = h_2 = h_3 = 1.5 \text{ m}$ (Fig. 7). The number of stacks is variable between $n = 1$

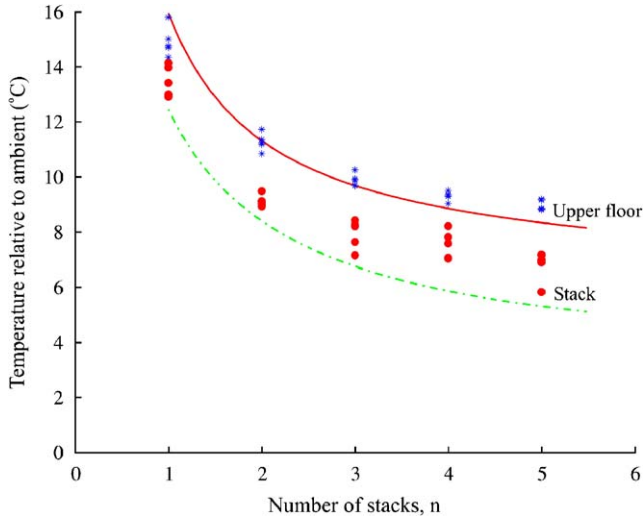


Fig. 11. Experimental data (symbols) and theoretical predictions (lines) of the steady state temperatures as the number of stacks, n is varied.

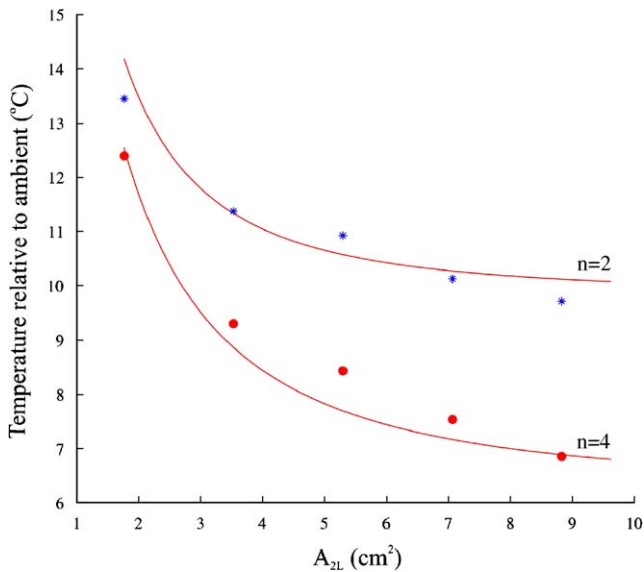


Fig. 12. Effect of variations in A_{2L} on the steady state temperatures. A_{2L} is increased from one to five openings with $A_{1L} = 3.5\text{ cm}^2$ (corresponding to two openings) fixed throughout. The number of stacks is also varied from $n = 2$ to 4.

and 5 where each is $x = 6.5\text{ m}$ tall and has a cross-sectional area of $A_S = 0.5\text{ m}^2$. The low level openings, A_{1L} and A_{2L} can be varied between 0 and 1 m^2 .

Firstly the effect of a variation in the number of stacks, n is considered where the inflow openings are fixed at $A_{1L} = A_{2L} = 0.5\text{ m}^2$. The volume fluxes Q_1 (corresponding to the basement) and Q_2 (corresponding to the ground floor) are plotted in Fig. 13 and the associated upper floor temperature in Fig. 14. As the number of stacks is increased the ventilation through both floors increases as a result of the larger area available for the flow. There are diminishing returns,

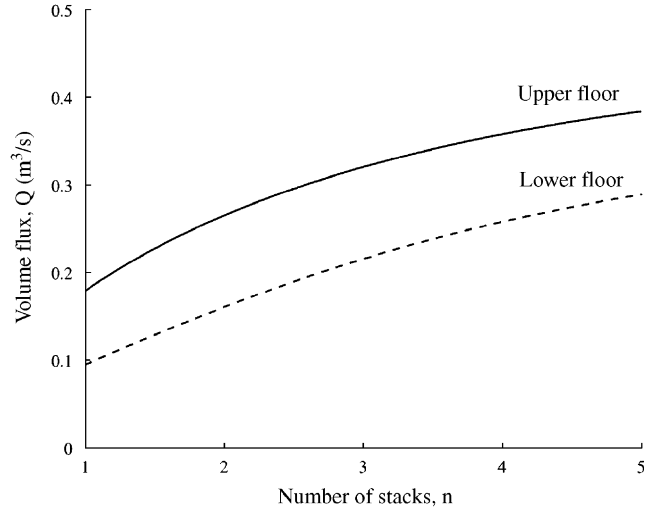


Fig. 13. Graphical solution of Eqs. (29) and (30) as the number of stacks, n is varied. In this example $A_{1L} = A_{2L} = 0.5\text{ m}^2$ and the upper floor witnesses a heat load of 3 KW.

however, as the number of stacks increases. When $n > 3$ the stack area becomes significantly greater than the low level openings A_{1L} and A_{2L} . Consequently A_{1L} and A_{2L} become the restricting areas to the flow and increasing n further has only a limited effect on the ventilation.

It is also useful to consider the variation in the magnitude of the ground floor heat flux. This is likely to vary significantly with the number of people on the floor or changes in solar radiation. As before, the low level openings are fixed at $A_{1L} = A_{2L} = 0.5\text{ m}^2$ whilst the number of stacks is constant at $n = 3$.

Figs. 15 and 16 show that the volume flux through both floors increases with the heat flux applied to the upper floor. The results from the single floor analysis of Section 2, where the ground floor is vented in isolation from the basement floor are also plotted. In this particular case, when the floors are coupled, the ventilation flow through the ground floor is approximately 20% lower than when it is uncoupled from the basement. This is due to the reduced buoyancy within the stack owing to the influx of ambient air from the basement. Consequently the temperature is around 1°C higher owing to the decreased advective heat loss from the ground floor.

This suppression of the ground floor flow, Q_2 by the induced basement flow is dictated by the magnitude of the opening, A_{1L} . In Fig. 17, the number of stacks is kept constant at $n = 3$ and the effect of the openings A_{1L} and A_{2L} on the flow is explored. At the far left of the figure, $A_{1L} = 0$, illustrating the case where the ground floor is vented in isolation, *upper (with lower blocked)*. As A_{1L} is opened, Q_1 increases owing to the increased area available for the flow. In doing so, however, Q_2 decreases due to the reduced buoyancy in the stack. If required, it is possible to adapt the flow areas to maintain the high flux through the second floor.

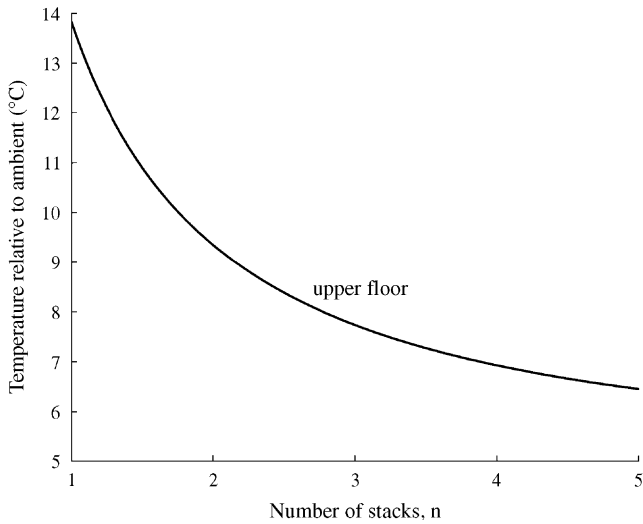


Fig. 14. The steady state temperatures relative to the ambient for $A_{1L} = A_{2L} = 0.5 \text{ m}^2$ as the number of stacks, n is varied.

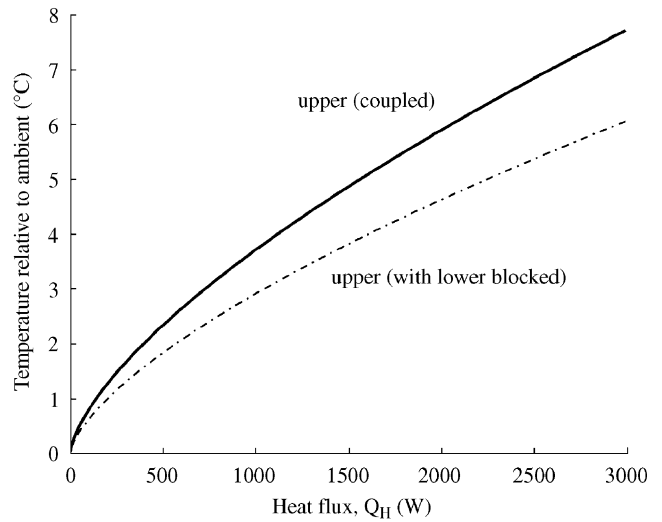


Fig. 16. The steady state temperature for $A_{1L} = A_{2L} = 0.5 \text{ m}^2$ with $n = 3$ stacks as the heat flux, Q_H is varied.

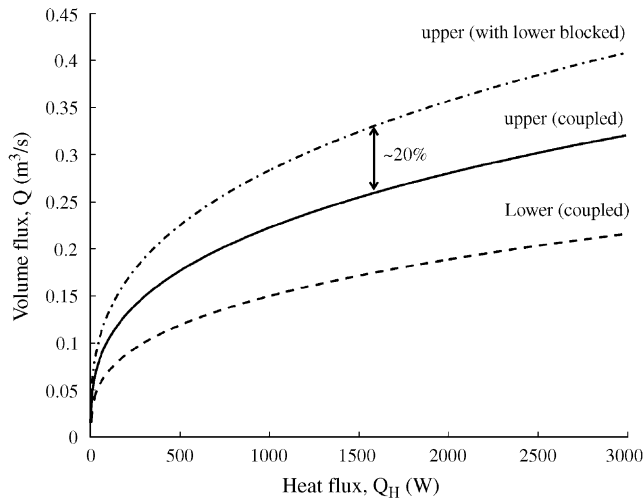


Fig. 15. The steady state volume flux for $A_{1L} = A_{2L} = 0.5 \text{ m}^2$ with $n = 3$ stacks as the heat flux, Q_H is varied.

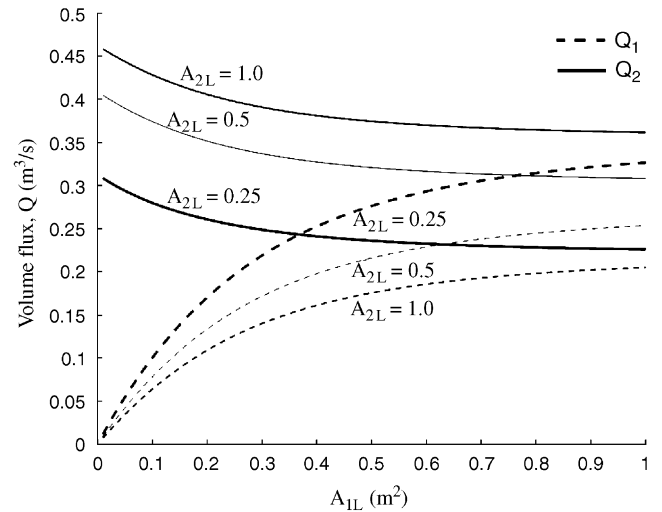


Fig. 17. Volume fluxes for variation in A_{1L} , with $n = 3$.

Consider the following scenario shown in Fig. 17 where initially $A_{1L} = 0$ and $A_{2L} = 0.25 \text{ m}^2$ such that $Q_2 \sim 0.3 \text{ m}^3/\text{s}$. A flow through the basement is required and A_{1L} is opened accordingly to 1 m^2 whilst A_{2L} is kept at 0.25 m^2 . With these flow areas the basement volume flux is $Q_1 \sim 0.32 \text{ m}^3/\text{s}$ whilst Q_2 drops to $0.22 \text{ m}^3/\text{s}$, a reduction of almost 30%. To maintain the original flow through the upper floor, A_{2L} is increased to 0.5 m^2 , thus increasing Q_2 to its former value whilst reducing Q_1 slightly to $0.26 \text{ m}^3/\text{s}$. Thus by careful consideration of the vent areas it is possible to provide an effective flow through the basement whilst maintaining the primary flow and temperature within the upper floor.

The size of the low level openings, A_{1L} and A_{2L} is instrumental to the relative magnitudes of the primary and secondary flows. The secondary flow is increased by opening A_{1L} , owing to the increased area for the flow. It

can also be increased by decreasing the size of the second floor opening A_{2L} . As A_{2L} is decreased, the flow through the ground floor is restricted which leads to a higher temperature within this floor. This warmer air flows into the stacks and provides a greater buoyancy to draw air through the basement. As the analysis has shown, however, inducing a greater flow through the basement will, if all else constant, reduce the primary flow. The flow through the ground floor can, however, be modified by consideration to the size of the opening on this floor, A_{2L} .

7. Conclusions

This study has investigated the use of stacks for the natural ventilation of buildings. By connecting the outflow from different spaces using common stacks,

buoyant air may be used to induce a secondary flow in a space with insufficient heat load to drive a flow. A model has been derived to predict the ventilation within an unheated low level floor coupled with a higher level heated floor. The model has been tested experimentally and the results are in close agreement with the theoretical predictions. The analysis has shown that the secondary ventilation increases with the ratio of the size of the openings between the lower to the upper floor and also the area of the stacks. In driving this secondary ventilation, however, the primary ventilation will be reduced, in some cases by as much as 20% and the steady state temperature increased by 1–1.5 °C. The reduction of the primary ventilation can be minimised, however, by careful design of the low level opening A_{1L} , ensuring that it is large enough to promote the secondary flow but not to the extent that it adversely effects the primary flow. Alternatively, the primary flow may be enhanced by opening up the upper inlet vent, A_{2L} .

Acknowledgements

This study was funded by the Cambridge-MIT Institute (CMI) and the BP institute for Multiphase Flow. The authors thank Charlotte Gladstone for helpful discussions.

Appendix A

A.1. Calculation of heat transfer coefficient

The magnitude of the heat transfer coefficient, U (W/m²K) for acrylic in water was determined using a transient cooling experiment. Initially, the upper (second) floor was filled with warm water at 30.9 °C and the outer tank (ambient) at 15.2 °C. All openings were sealed and the stacks blocked. The tank was then left for 3.5 h, over which time the internal temperature and ambient temperature were logged (Fig. 18).

The steady state heat loss, Q_L through acrylic may be given by

$$Q_L = UA_R(T - T_E), \quad (35)$$

where A_R is the surface area of the floor in contact with the ambient water (~0.16 m²). To evaluate U the heat loss, Q_L from (35) is equated to the change in internal energy of the water within the sealed floor (of mass m) as it cools = $-mC_p \frac{dT}{dt}$ to give in the form of Newton's law of cooling as

$$\frac{dT}{dt} = -K(T - T_E), \quad (36)$$

where

$$K = \frac{UA_R}{mC_p}. \quad (37)$$

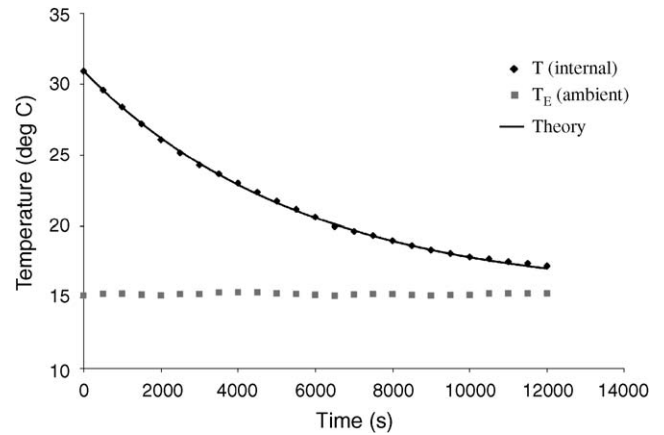


Fig. 18. Transient heat loss experiment, showing the temperature in the upper floor, T , the theoretical prediction (Eq. (39)) and also the ambient temperature T_E .

To simplify the analysis it is assumed that there is a linear temperature gradient across the acrylic. Under the initial conditions $T = T_{\text{initial}}$ at $t = 0$ Eq. (36) has the solution

$$T = T_E + (T_{\text{initial}} - T_E)e^{-Kt}. \quad (38)$$

By substituting experimental values from Fig. 18, Eq. (38) can be expressed as

$$T = 15.2 + 15.73e^{-1.78 \times 10^{-4}t}. \quad (39)$$

This curve has been plotted in Fig. 18 (solid line) and shows good accord with the experimental data. The heat transfer coefficient is therefore given by rearranging (37) as

$$U = \frac{mC_p K}{A_R} = 13 \text{ W/m}^2\text{K}. \quad (40)$$

For a temperature difference of 15 °C between the upper floor and the ambient we can expect a heat loss of around 30 W. Under a heat load of 450 W, this equates to a 7% loss in energy. Under lower temperature variations, however, Q_L decreases sharply and becomes less significant.

A.2. Model for time to adjust to steady state

Following Chenvidyakarn and Woods, [6] a dimensional timescale for the converge to steady state, t_s may be given by

$$t_s = \frac{V(\rho C_p)^{1/3}}{A^{*2/3} (g\alpha h_3)^{1/3} Q_H^{1/3}}, \quad (41)$$

where V is the volume of the space and A^* the effective area of A_{2L} and A_{2U} . By applying the appropriate values of geometry from the apparatus in Fig. 4 and for a typical experiment where $A_{2L} = 3.5 \text{ cm}^2$, $A_{2U} = 3.1 \text{ cm}^2$

Table 1

Symbol	Property	Value (if applicable)
c	Discharge coefficient through openings (dimensionless)	0.7
C_p	Specific heat capacity	4200 J/KgK (water) & 1007 J/KgK (air)
f	Friction factor for flow in stacks	–
g	Acceleration due to gravity	9.81 m/s ²
Re	Reynolds number	–
U	Heat transfer coefficient	For acrylic in water $U = 13$ W/m ² K
α	Thermal expansion coefficient	0.0002 1/K (water) & 0.0035 1/K (air)
ν	Kinematic viscosity	10 ⁻⁶ m ² /s (water) 10 ⁻⁵ m ² /s (air)
K	Constant of proportionality (Newton's law of cooling)	1.78 × 10 ⁻⁴ 1/s

Table 2

Symbol	Property
A_L	Area of low level opening
A_U	Area of opening into stack
A_S	Cross-sectional area of each stack
n	Number of stacks (1–5)
H	Height of floor between inlet vent and entrance to stack
x	Height of stack
ΔP_L	Pressure loss through lower opening
ΔP_U	Pressure loss through stack entry
ΔP_M	Pressure loss in stack turning
$\Delta P_{friction}$	Frictional pressure loss in stack
T	Temperature of fluid in floor
ρ	Density of fluid in floor
T_E	Temperature of ambient fluid
ρ_E	Density of ambient fluid
Q_H	Heat load in floor
A_R	Surface area in floor (inc. walls and ceiling)
Q_L	Volume flux through lower opening
Q_U	Volume flux into stack ($Q_L = Q_U = Q$)
u	Velocity flux up stack
\dot{m}	Mass flux up stack
m	Mass of fluid in upper floor
P_U	Pressure inside entrance to stack
P_D	Pressure at base of control volume
P_S	Pressure at top of control volume

(corresponding to two stacks) and $Q_H = 450$ W, a time constant of $t_s \sim 6$ min is obtained. Typically the convergence to steady state is achieved within $3.5t_s$, [6] which shows that the time of 20 min found in the experiments is appropriate. The same approach can be applied to a full scale building using the geometry of the example building given in Section 6. For a volume of $V = 250$ m³, the analysis suggests that the temperature and ventilation flow will reach steady state conditions within 45 min.

A.3

Physical constants and dimensionless numbers are shown in Table 1.

Table 3

Symbol	Property
A_{1L}, A_{2L}	Area of first and second floor low level openings
A_{1U}, A_{2U}	Area of first and second floor stack openings (each stack)
A_R	Surface area in second floor
h_1	Height from first floor inlet to first floor stack entrance
h_2	Height from first floor stack entrance to second floor low level inlet
h_3	Height from second floor inlet to second floor stack entrance
$\Delta P_{1L}, \Delta P_{2L}$	Pressure loss through low level openings
$\Delta P_{1U}, \Delta P_{2U}$	Pressure loss through stack entrance (for n stacks)
$\Delta P_{M(2)}$	Pressure loss in stack at second floor inlet
$\Delta P_{fric(1)}, \Delta P_{fric(2)}$	Frictional pressure losses below and above second floor stack entry
T_2	Temperature in second floor
ρ_2	Density in second floor
T_M	Temperature of fluid in stack (above second floor inlet)
ρ_M	Density of fluid in stack (above second floor inlet)
T_E	Temperature of ambient fluid
ρ_E	Density of ambient fluid
Q_H	Heat load in second floor
u_1, u_2	Velocity fluxes through first and second floors
Q_1, Q_2	Volume fluxes through first and second floors ($Q_3 = Q_1 + Q_2$)
m	Mass of fluid in upper floor
P_U	Pressure inside entrance to stack
P_D	Pressure at base of control volume
P_S	Pressure at top of control volume

A.4

Variables used in single floor analysis are shown in Table 2.

A.5

Variables used in two floor analysis are shown in Table 3.

References

- [1] Building Research Establishment, Selecting air conditioning systems, Good Practice Guide, No. 71.
- [2] Fitzgerald SD, Woods AW. Natural ventilation of a room with vents at multiple levels. *Building and Environment* 2004;39:505–21.
- [3] Gladstone C, Woods AW. On buoyancy-driven natural ventilation of a room with a heated floor. *J Fluid Mechanics* 2001;441:293–314.
- [4] Holford JM, Hunt GR. Fundamental atrium design for natural ventilation. *Building and Environment* 2003;38:409–26.
- [5] Short CA, Lomas KJ, Woods AW. Design strategy for low-energy ventilation and cooling within an urban heat island. *Building Research Information* 2004;32(3):187–206.
- [6] Chenvidyakarn TB, Woods AW. Multiple steady states in stack ventilation. *Building and Environment* 2005;40:399–410.
- [7] Turner JS. Buoyancy effects in fluids. Cambridge: Cambridge University Press; 1973.
- [8] Li Y, Delsante A. Natural ventilation induced by combined wind and thermal forces. *Building and Environment* 2001;36:59–71.
- [9] Etheridge D, Sandberg M. Building ventilation, theory and measurement. New York: Wiley; 1996.
- [10] Linden PF, Lane-Serff GF, Smeed DA. Emptying filling boxes: the fluid mechanics of natural ventilation. *J Fluid Mechanics* 1990;212:300–35.
- [11] Douglas JF, Gasiorek JM, Swaffield JA. Fluid mechanics. New York: Longman Scientific and Technical; 1986.
- [12] Batchelor GK. An introduction to fluid mechanics. Cambridge: Cambridge University Press; 1967.
- [13] Ward-Smith AJ. Internal fluid flow, The fluid dynamics of flow in pipes and ducts. Oxford: Clarendon Press; 1980.
- [14] Press WH, Flannery BP, Teukolsky SA, Vetterling WT. Numerical recipes. Cambridge: Cambridge University Press; 2002.